Journal of Engineering and Applied Sciences 14 (Special Issue 4): 7290-7296, 2019
ISSN: 1816-949X

Fabrication and Properties of Ag_2O/Si Heterojunction Solar Cell Pure and Doped (Sb, Sn and Se)

[1]Bushra H. Hussein, [1]Hanan K. Hassun, [1]Bushra K.H. Al-Maiyaly, [2]Kadhim A. Aadim and [1]Tagreed M. Al-Saadi
[1]Department of Physics, College of Education For Pure Science (Ibn Al-Haitham),
[2]Department of Physics, College of Science, University of Baghdad, Baghdad, Iraq
bushrahhz@yahoo.com, dr.bushra2009@yahoo.com, kdhim_adem@scbaghdad.edu.iq,
tagreedmm2000@gmail.com

Abstract: Ag_2O thin film has been deposited pure and doped with Sb, Sn and Se with thickness about 500 nm by utilizing thermal oxidation during 750 K with ambient oxygen of silver (Ag) thin films that deposited in a vacuum on a glass substrate and Si wafer to manufactory (p-Ag_2O/n-Si) heterojunction for photovoltaic devices. The influence of Sb, Sn and Se with ratio 3% dopants on the optical, structural and electrical properties of Ag_2O thin film and studied the main parameters of solar cells for p-Ag_2O/n-Si heterojunction. The sample p-Ag_2O/n-Si: Se with a band gap of 1.7 eV for show efficiency of solar cell 4.25% with V_{oc}0.35V, J_{sc} 22 mA/cm^2 and FF 0.55 compared with the samples doped with Sb and Sn.

Key words: p-Ag_2O/n-Si, doping Sb, Sn and Se, thin films, solar cell, silver

INTRODUCTION

Silver Oxide (Ag_2O) is direct band gap and p-type semiconductor that is used in optical memory, photography and solar energy converters converters (Barik *et al*., 2003). Several techniques have been utilize to produce Ag_2O films, thermal evaporation evaporation (Pettersson and Snyder, 1995), anodic oxidation of Ag and furnace thermal (Hecht *et al*., 1996), reactive electron beam, RTO technique using halogen lamp (Ismail *et al*., 2005), chemical bath deposited (Nwanya *et al*., 2013), DC magnetron sputtering (Hajakbari and Ensandoust, 2016), gas plasma oxidation of thermally evaporated (Ovchinnikov, 2016), rapid thermal oxidation (Muhsien and Hamdan, 2012).

Silver-Oxygen system (Ag-O) exists in different compounds, namely: AgO, Ag_2O, Ag_2O_3, Ag_3O_4, Ag_4O_3 and Ag_4O_4. The most thermodynamically stable among these oxides is Ag_2O. It owns a simple cubic structure at RT (Pierson and Rousselot, 2005). Silver oxide thin film is a p-type semiconductor with a band gap (1.2-3.4 eV) due to the crystallinity of structure, phases and physical properties arising from the employed grow technique (Gao *et al*., 2010). The purpose of the present research is the fabrication of the solar cell of p-Ag_2O/n-Si heterojunction and investigation of the influence of different dopants material (Sb, Sn and Se) on the main parameters of solar cell and on characteristics of Ag_2O thin films were deposited by thermal evaporation technique at room temperature on glass and silicon substrates.

MATERIALS AND METHODS

Experimental: High purity for silver film was deposited on a single crystal Si wafer of n-type conductivity with (111) orientation, indirect energy, a gap of 1.1 eV and resistivity 1-5 Ω.cm of 500 nm thickness for photovoltaic application and on glass slides in order to study the electrical, structural and optical properties of Ag_2O thin films by using the Edward coating unit model (E 306) system of 3×10^{-6} Torr where the technique was thermal evaporation at RT. Ag_2O film was gotten with assistance of thermal oxidation at 750 K with ambient oxygen flow with the rate (500 sccm) for 2 h. Then the films were doping with different pure element (99.999% of Se, Sn and Sb) with atomic percentages 0.3 wt.% by thermal diffusion 473 K for 1 h. It was using an optical interferometer method to determine the thickness of films.

X-Ray Diffraction XRD and Atomic Force Microscopy (AFM) techniques have characterized the structural morphology of the Ag_2O films. The optical transmission measurements in the range of (400-1100 nm) were done by UV/visible 1800 spectrophotometer.

Corresponding Author: Bushra H. Hussein, Department of Physics, College of Education For Pure Science (Ibn Al-Haitham), University of Baghdad, Baghdad, Iraq, bushrahhz@yahoo.com

The type of carrier, concentrations and their mobility were measured by Hall effect studies using the van der Pauw-Ecopia HMS-3000. The 1-5 characteristics of the Ag_2O/n-Si heterojunction were measured using (F30-2, Farnell Instrument) and (Keithley Digital Electrometer 616), the measurements were performed under light with intensities 100 mW/cm^2. The I_{sc}, V_{oc}, fill factor FF and photovoltaic conversion efficiency values for all heterojunctions solar cells were determined, the carrier life time was measured by (Digital storage Oscilloscope-Twintex-TSO 1202) 200 MHz.

RESULTS AND DISCUSSION

Figure 1a-c displays the XRD patterns of the deposited Ag_2O thin films with a thickness (500 nm) pure and doping with (Sb, Sn and Se), the patterns show that all thin films pure and doped with Sb, Sn and Se have a polycrystalline with cubic phases and strongest sharp peak corresponding to (111) at diffraction angle 38.11, all the peaks of diffraction can be assigned to Ag_2O (ICDD003-0796). Another one noticeable peak (200) when diffraction angle 46.2 can observe. We can notice when adding the doping atoms (Sb, Sn and Se) the places for measured diffraction peaks do not alteration significantly but the intensities peaks increase with doping and crystallite size become larger and this depended on ion size differences among Ag and other doping atoms (Sb, Sn and Se).

The crystallites size estimated by Scherer's formula (Omer, 1975) is listed in Table 1 where it shows that the sample Ag_2O:Se have high crystallite size from other samples because of the relatively small atom (ionic radius of Se 0.56 Å) (Shannon, 1976; Sethi and Satake, 1992) doping entering into the lattice structure and moving to interstitial positions in the Ag_2O. The X-ray spectra of the pure and doping films are observed in Fig. 1 it appears that there are few shifts in the positions of peaks (2θ) for prepared films after doping presses. This displacement due to simple stress arising from the doping atom entry and its site occupation in its crystal lattice (Bouville, 2004). It is known that the doping effective effect of in semiconductors occurs when the ionic diameter of doping atoms are smaller or equal to the host material (Shannon, 1976).

The surface morphology of the pure Ag_2O thin films and doped with (Sb, Sn and Se) was examined by AFM analysis. Figure 2 shows granularity cumulation distribution chart and three dimensional AFM images of these films. The small particles have grown on the substrate surface and the pyramidal morphology variations can be seen. The observed physical dimensions of the structure such as average Grain Size (GS), roughness and root mean square are listed in Table 2, the structures varied in average grain size from

Table 1: Structural parameters of Ag_2O with different impurity (Sb, Sn and Se) thin films

Thickness (500 nm)	2θ(°)	d_{hkl}(Exp.)(Å)	β(°)	C_S(nm)
Pure Ag_2O	38.11	2.35	0.1480	59.31
Ag_2O: Sb	38.10	2.35	0.1426	61.81
Ag_2O: Sn	38.09	2.36	0.1335	65.75
Ag_2O: Se	38.07	2.36	0.1321	66.44

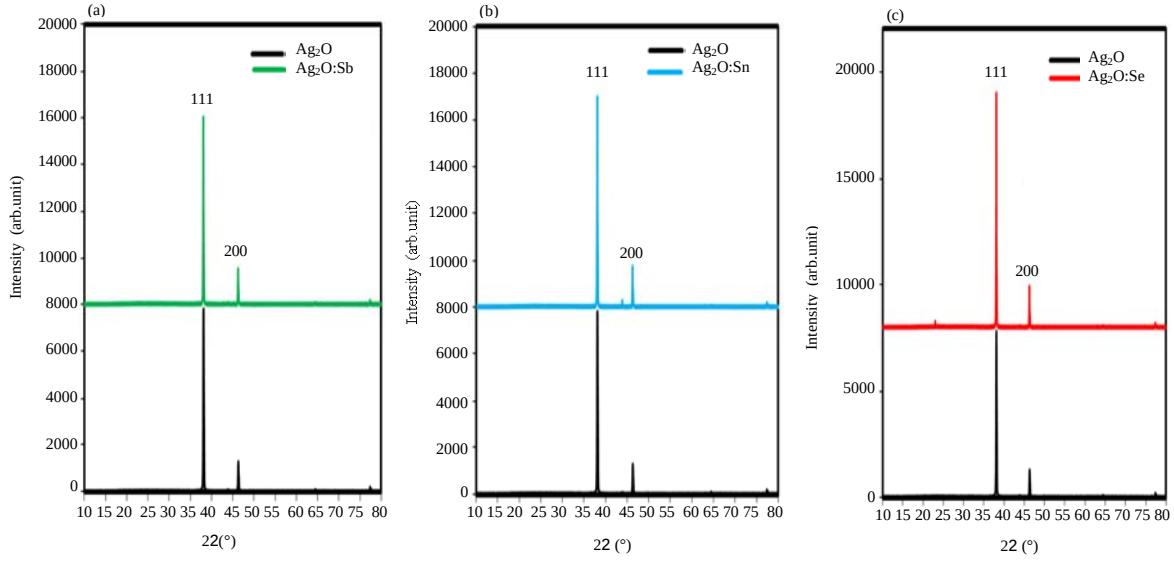

Fig. 1: a-c) XRD patterns for thin Ag_2O films with different impurity (Sb, Sn and Se)

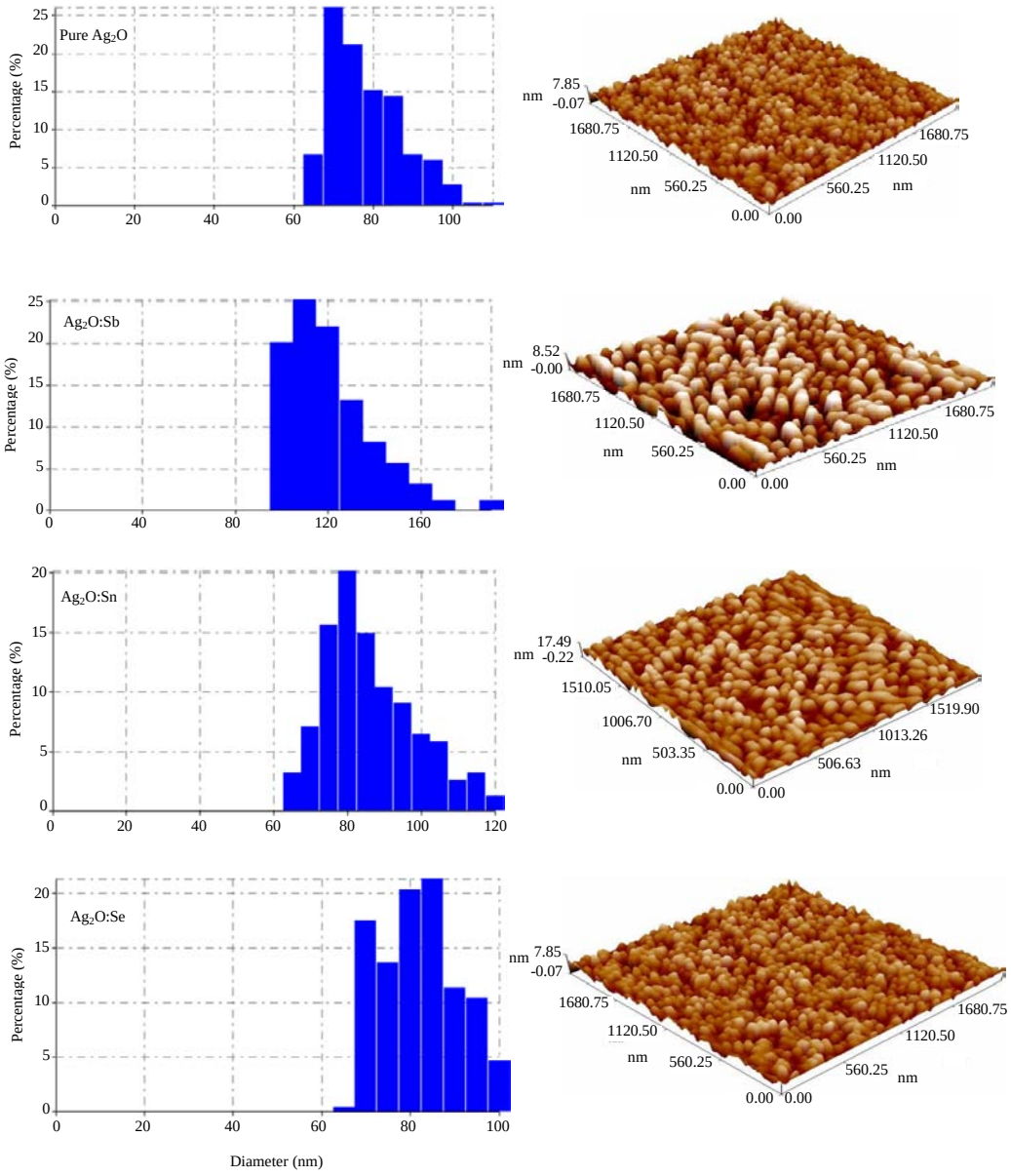

Fig. 2: Granularity cumulation distribution chart and three dimension atomic force microscopy of Ag_2O as and dopant atoms (Sb, Sn and Se)

Table 2: The grain size, roughness average and root mean square of Ag_2O with different impurity (Sb, Sn and Se) thin films

Thickness (500nm)	Grain Size (GS) (nm)	Roughness average (nm)	RMS (nm)
Pure Ag_2O	75.93	1.04	1.25
Ag_2O: Sb	79.67	2.13	2.46
Ag_2O: Sn	83.96	2.37	2.84
Ag_2O: Se	115.64	4.51	5.21

(75.93-115.64 nm) as well as to the variations in the roughness and root mean square values. It is clear from this Table 2 the average grain size, roughness and root mean square are increased after doping Ag_2O thin film and the sample Ag_2O:Se have high values. This behavior is due to the increase of the mobility of the atoms which causes the agglomeration of particles and of larger particles which in turn clues to a rise of the film roughness. These observations agree with XRD results.

The transmittance and reflection spectra of the pure Ag_2O films and doping with different impurity atoms (Sb, Sn and Se) in the wavelength range of (400-1100 nm)

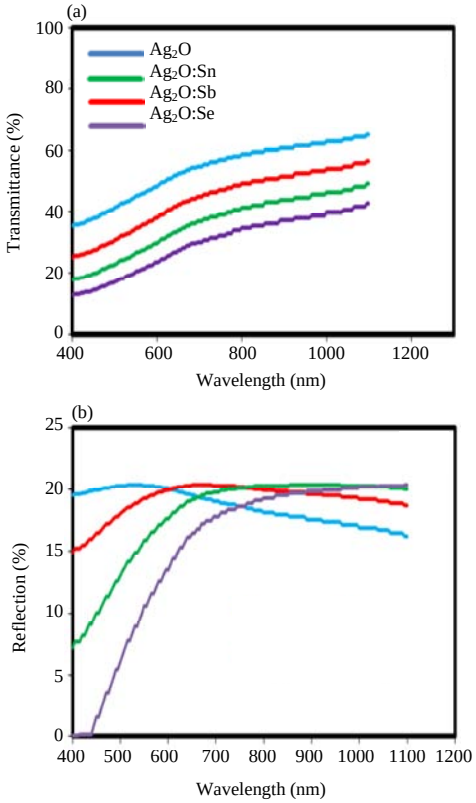

Fig. 3: a, b) The transmittance and reflection spectrum of Ag_2O thin films and dopant atoms (Sb, Sn and Se)

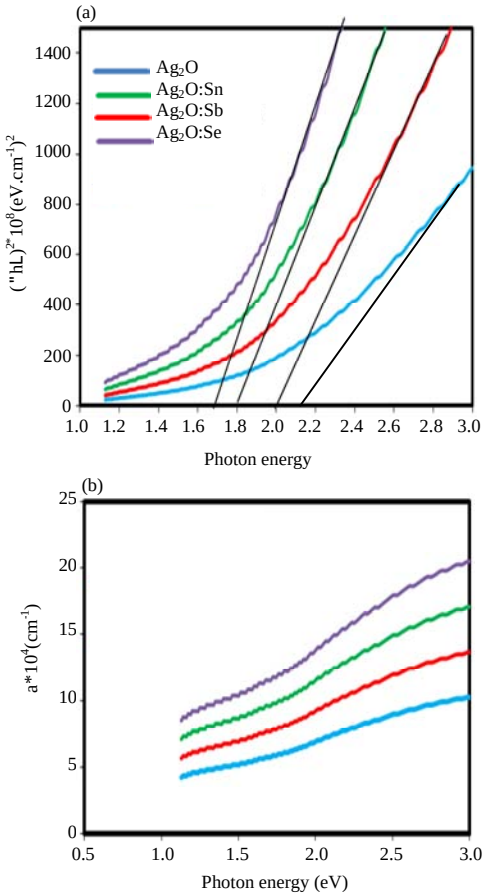

Fig. 4: a) The $(\alpha h\upsilon)^2$ with photon energy E_g and b) Absorption coefficient with photon energy Eg of Ag_2O and dopant atoms (Sb, Sn and Se)

are displayed in Fig. 3a, b. It can be seen that the transmittance values decrease when adding impurity atoms (Sb, Sn and Se) which means after doping the absorbance values for these thin films are increasing, the photons absorption by free carrier contributed to the decrease in optical transmittance or might be attributable to the growth of the crystallite size (Tigau *et al*., 2003). It is clear from (Fig. 3b) that the reflectance values of prepared Ag_2O thin films pure and doped are below 20%, these low values make these films a desired material for photovoltaic application. Ag_2O:Se film has the lowest values below 10% when the range of wavelength (400-700 nm) this behavior can be related to XRD and AFM data to understand the correlation between surface morphology and the reduction in reflectance.

The Tauc equation was used to calculate the energy gap (Khudayer *et al*., 2018). It is appraised from the extrapolation to zero absorption in the Tauc equation. The variation of Eg with pure Ag_2O and different impurity (Sb, Sn and Se) is illustrated in Fig. 4a. The allowed direct transition optical energy gaps of (Ag_2O) films were calculate to 2.15 eV good agreement with (Nwanya *et al*., 2013; Muhsien and Hamdan, 2012; Gao *et al*., 2010; Chopra and Malhota, 1985) while lie in the range (2-1.7 eV) for the films doped with different impurity (Sb, Sn and Se), this means it is decreased after doping this decreed due to the dopant atoms at the grain boundaries and more absorbance can be get in Ag_2O:Se films, Se introduces some extra energy levels in the Ag_2O band gap near to the valence band edge with a resultant reduction of the energy connected with direct transition. The absorption coefficient α calculated from exponential law the Urbach law which it is expressed by Omer (1975). In this present study the α values before and after doping with different

Table 3: Allowed direct optical band gap and absorption coefficient of Ag_2O with different impurity (Sb, Sn and Se) thin films

$\lambda = 500$ nm

Thickness (500 nm)	E_g^{opt}(eV)	$\alpha \times 10^4$ cm^{-1}
Pure Ag_2O	2.15	8.9
Ag_2O: Sb	2.00	11.8
Ag_2O: Sn	1.80	15.0
Ag_2O: Se	1.70	18.0

impurity (Sb, Sn and Se) show in Table 3, the high value is 18×10^{4} cm^{-1} for Ag_2O:Se. These values indicate the increasing of localized states in the band gap after the doping (Table 4 and 5).

To find the film type (n or p), carrier concentrations, mobility and resistivity of Ag_2O pure and (Sb, Sn and Se) doped thin films it should estimate the Hall effect as show in Table 4, it can see the electrical resistivity of doped Ag_2O thin films is lower than that of the pure thin film due to the free holes released by the substitution of doping atoms orions at the sites occupied by Ag ions. The positive sign of the $R_{(H)}$ shows that the conductivity of the film is p-type, similar behaves was obtained by Nwanya *et al.* (2013). The carrier concentration $10^{17}cm^{-3}$ orders is in a good contract with the research (11). It can notice from Table 4 that the mobility and concentration rises after doping with different impurity (Sb, Sn and Se), this designate that the development in the film structure and decrease grain boundary scattering (Fig. 5 and 6).

Table 4: Hall parameters of Ag_2O pure and doped with different impurity (Sb, Sn and Se) thin films

Thickness (500 nm)	$R_{(H)}$	n (cm-3)*10^{17}	μ_H(cm^2/VS)	ρ(Ω.cm)
Pure Ag_2O	7.102273	8.80	11.45528	1.612903
Ag_2O: Sb	6.756757	9.25	17.78094	2.631579
Ag_2O: Sn	5.161024	12.11	18.43223	3.571429
Ag_2O: Se	4.191818	14.91	41.09625	9.803922

Table 5: The parameters of solar cell for Ag_2O/Si heterojunction for pure and different dopant (Sb, Sn and Se)

Thickness (500 nm)	V_{oc} (Volt)	J_{sc} (mA/cm^2)	V_{max} (Volt)	J_{max} (mA/cm^2)	FF	η (%)
Pure Ag_2O	0.25	9	0.15	5	0.333333	0.75
Ag_2O: Sb	0.30	13	0.18	8	0.369231	1.44
Ag_2O: Sn	0.31	16	0.20	13	0.524194	2.60
Ag_2O: Se	0.35	22	0.25	17	0.551948	4.25

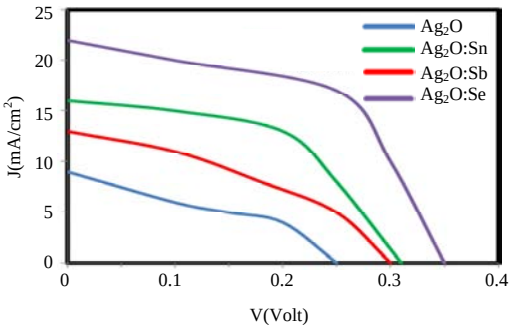

Fig. 5: The 1-5 characteristic for Ag_2O/Si solar cell under illumination for pure and different dopant (Sb, Sn and Se)

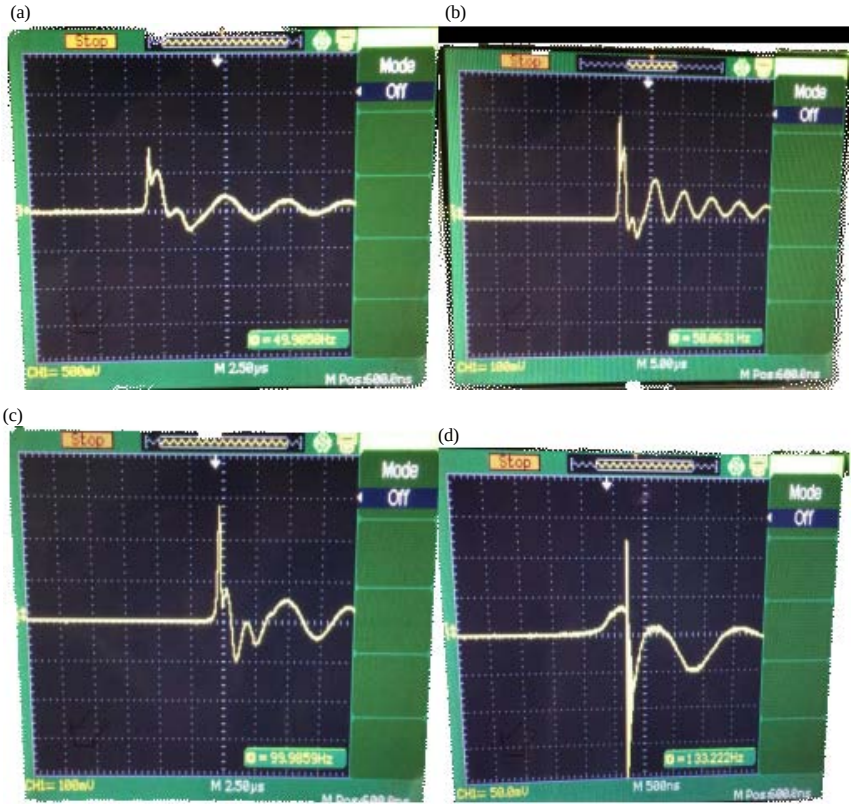

Fig. 6: The carrier lifetime of Ag_2O/Si for pure and different dopant (Sb, Sn and Se): a) Pure Ag_2O; b) Ag_2O:Sb; c) Ag_2O:Sn and d) Ag_2O:Se

Figure 5 and Table 5, illustration the current voltage 1-5 characteristics of fabricated Ag_2O/Si heterojunction and dopant atoms (Sb, Sn and Se) under illumination condition in the forward direction (Sze and Ng, 2006). The results obtained shows the efficiency increases in general with different impurity (Sb, Sn and Se) and this return to increase in the charge carriers, surface roughness, the absorption coefficient, the Ag_2O:Se cause interface atoms rearrangement and the reducing of the surface states and dangling bond which leads to improve of the junction characteristics. It can distinguish the direct relation between J_{SC} and V_{OC} when the incident photo power (100 mW/cm^2) from the J-V curve, the total separation of the photo-generated electron-hole pairs. This behavior of V_{OC} and J_{SC} refers to the perfect linearity of the prepared device to work as a solar cell.

The carrier lifetime of the Ag_2O/Si heterojunction was calculated based on the rise time rise of the output signal from the exposed junction to the pulse laser under a 5 V reverse bias as shown in Fig. 6. The highest carrier life time is obtained when Ag_2O: Se.

CONCLUSION

Thin films of polycrystalline Ag_2O pure and doped with a different dopant (Sb, Sn and Se) are prepared by the thermal oxidation method and their application to p-Ag_2O/n-Si heterojunction solar cell were examined. XRD and AFM studies reveal that the doping Ag_2O with (Sb, Sn and Se) strongest effects on the structural and morphology of the films as well as the crystallites size and the average grain size increase after doping. Hall data revealed no change in type of carrier after doping with increase either carrier concentration or mobility. Ag_2O films display good absorption in the spectral range (400-700 nm). Heterojunction p-Ag_2O/n-Si solar cell exhibited good rectifying characteristics; the solar cell efficiency was enhanced after doping. A remarkable improvement in performance of solar cells for sample which doping with Se, the efficiency of this solar cell might be increased with increase doping concentration with Se.

REFERENCES

Barik, U.K., S. Srinivasan, C.L. Nagendra and A. Subrahmanyam, 2003. Electrical and optical properties of reactive DC magnetron sputtered silver oxide thin films: Role of Oxygen. Thin Solid Films, 429: 129-134.

Bouville, M., 2004. The role of stress and diffusion in structure formation in semiconductors. Ph.D Thesis, University of Michigan, Ann Arbor, Michigan.

Chopra, K.L. and L.K. Malhota, 1985. Optical Properties of Thin Films. Tata McGraw-Hill, New Delhi, India.

Gao, X.Y., H.L. Feng, J.M. Ma, Z.Y. Zhang and J.X. Lu *et al*., 2010. Analysis of the dielectric constants of the Ag_2O film by spectroscopic ellipsometry and single-oscillator model. Phys. B. Condens. Matter, 405: 1922-1926.

Hajakbari, F. and M. Ensandoust, 2016. Study of thermal annealing effect on the properties of silver thin films prepared by DC magnetron sputtering. Acta Phys. Pol. A., 129: 680-682.

Hecht, D., P. Borthen and H.H. Strehblow, 1996. An X-ray absorption fine structure study of the initial stages of the anodic oxidation of silver. Surf. Sci., 365: 263-277.

Ismail, R.A., K.Z. Yahya and O.A. Abdulrazaq, 2005. Preparation and photovoltaic properties of Ag_2O/Si isotype heterojunction. Surf. Rev. Lett., 12: 299-303.

Khudayer, I.H., B.H.H. Ali, M.H. Mustafa and A.J. Ibrahim, 2018. Investigation of the structural, optical and electrical properties of agInSe2 thin films. J. Pure Appl. Sci., 31: 37-49.

Muhsien, M.A. and H.H. Hamdan, 2012. Preparation and characterization of p-Ag_2O/n-Si heterojunction devices produced by rapid thermal oxidation. Energy Procedia, 18: 300-311.

Nwanya, A.C., P.E. Ugwuoke, B.A. Ezekoye, R.U. Osuji and F.I. Ezema, 2013. Structural and optical properties of chemical bath deposited silver oxide thin films: Role of deposition time. Adv. Mater. Sci. Eng., 2013: 1-8.

Omer, M.A., 1975. Elementary Solid State Physics. Pearson, London, UK., ISBN:978-81-7758-377-9, Pages: 673.

Ovchinnikov, V., 2016. Reduction of silver oxide film in inert gas plasma. Proceedings of the 10th International Conference on Quantum, Nano/Bio and Micro Technologies (ICQNM), July 24-28, 2016, IARIA Publisher, New York, USA., pp: 6-11.

Pettersson, L.A.A. and P.G. Snyder, 1995. Preparation and characterization of oxidized silver thin films. Thin Solid Films, 270: 69-72.

Pierson, J.F. and C. Rousselot, 2005. Stability of reactively sputtered silver oxide films. Surf. Coat. Technol., 200: 276-279.

Sethi, M.S. and M. Satake, 1992. Periodic Tables and Periodic Properties of the Elements. Discovery Publishing House, Delhi, India.

Shannon, R.D., 1976. Revised effective ionic radii and systematic studies of interatomic distances in halides and chalcogenides. Acta Crystallogr., 32: 751-767.

Sze, S.M. and K.K. Ng, 2006. Physics of Semiconductors Devices. 3rd Edn., Wiley Publishing Company, Hoboken, New Jersey, USA., ISBN:978-0-471-14323-9, Pages: 832.

Tigau, N., V. Ciupina, G. Prodan, G.I. Rusu and C. Gheorghies *et al*., 2003. The influence of heat treatment on the electrical conductivity of antimony trioxide thin films. J. Optoelectron. Adv. Mater., 5: 907-912.